

Polymer Chemistry

Accepted Manuscript



This is an *Accepted Manuscript*, which has been through the Royal Society of Chemistry peer review process and has been accepted for publication.

Accepted Manuscripts are published online shortly after acceptance, before technical editing, formatting and proof reading. Using this free service, authors can make their results available to the community, in citable form, before we publish the edited article. We will replace this *Accepted Manuscript* with the edited and formatted *Advance Article* as soon as it is available.

You can find more information about *Accepted Manuscripts* in the [Information for Authors](#).

Please note that technical editing may introduce minor changes to the text and/or graphics, which may alter content. The journal's standard [Terms & Conditions](#) and the [Ethical guidelines](#) still apply. In no event shall the Royal Society of Chemistry be held responsible for any errors or omissions in this *Accepted Manuscript* or any consequences arising from the use of any information it contains.

ARTICLE

Exploring the homogeneous controlled radical polymerisation of hydrophobic monomers in anti-solvents for their polymers: RAFT and ATRP of various alkyl methacrylates in anhydrous methanol to high conversion and low dispersity.

Cite this: DOI: 10.1039/x0xx00000x

Received 00th January 2012,
Accepted 00th January 2012

DOI: 10.1039/x0xx00000x

www.rsc.org/

A. B. Dwyer, P. Chambon, A. Town, F. L. Hatton, J. Ford and S. P. Rannard*

In previous reports, the use of anhydrous methanol in the homogeneous ATRP polymerisation of *n*-butyl methacrylate (*n*BuMA) was shown to yield polymers with dispersities as low as $\mathcal{D} = 1.02$, despite methanol being widely regarded as an anti-solvent for *p*(*n*BuMA). Herein, we describe the homogeneous methanolic controlled radical polymerisation of three hydrophobic alkyl methacrylate monomers (methyl, *t*-butyl and *n*-butyl methacrylate) using both ATRP and RAFT to generate a range of homopolymers, statistical copolymers, amphiphilic block copolymers and branched polymers. Methanolic ATRP and RAFT are compared, with RAFT able to target high degrees of polymerisation (800 monomer units) with very low dispersities ($\mathcal{D} = 1.06$) in shorter reaction times (44 hrs) under these conditions. Poly(ethylene glycol)-derived macroinitiators were shown to generate well defined A-B and A-B-A block copolymers ($\mathcal{D} = 1.02$ -1.18) whilst branched A-B block copolymers with weight average molecular weights up to $M_w = 2.33 \times 10^6$ g/mol were readily synthesised. The role of methanol within the polymerisations is discussed.

Introduction

The control of polymer syntheses to generate defined molecular weight materials with narrow dispersity (\mathcal{D}), high yield, high conversion, bespoke functionality and complex macromolecular architecture is an ongoing theme globally.¹ To ensure success, conditions such as initiator chemistry, catalyst choice, ratio of reagents, solvent environment, reaction temperature and concentration must be studied and optimised;¹⁻⁵ in many cases this is required on a monomer-to-monomer and polymerisation technique basis. Polymer purification and recovery often requires at least one precipitation step into an anti-solvent and, for many years, methanol (MeOH) has been the anti-solvent of choice for hydrophobic polymers.⁶ Such precipitation may provide poor removal of unreacted initiator fragments⁷ and lead to fractionation of the molecular weight distribution, through the increased solubility of oligomers and low molecular weight chains, however this is often ignored and analysis of the recovered polymer is used to determine the overall polymerisation outcome using techniques such as ¹H nuclear magnetic resonance spectroscopy (NMR).⁷

Alcohols and alcohol/water mixtures have also been shown to aid the control of some atom transfer radical polymerisation (ATRP) reactions, with MeOH frequently featuring in the successful control of various hydrophilic methacrylate monomers. Examples include oligo(ethylene glycol) methyl ether methacrylate,^{8a} 2-hydroxyethyl methacrylate,^{8b} 2-(dimethylamino)ethyl methacrylate^{8c} and glycerol methacrylate,^{8d} whilst alcohols may vary from MeOH to ethanol, propanol and isopropanol (IPA). In several cases, transesterification of hydrophilic methacrylates with alcoholic solvents has been reported⁹ to various extents under ATRP conditions, dependent on the structure of the chosen solvent.¹⁰

The controlled polymerisation of hydrophobic monomers in alcohols and alcohol/water mixtures is of particular interest as they: 1) are relatively cheap, 2) may reduce the use of high boiling solvents (exothermic reactions are often conducted at reflux or utilise complex temperature control systems in industry),^{11a} 3) avoid the potential formation of explosive oxidation products (eg peroxides in tetrahydrofuran), and 4) are considered to present relatively low health and environmental hazards.^{11b} Maintaining truly homogeneous reactions under

these conditions is difficult if the final polymer is insoluble in the protic solvent environment at high conversion. Some years ago, we reported the use of IPA and IPA/water mixtures to polymerise *n*-butyl methacrylate (*n*BuMA) under Cu(I) catalysed, ambient ATRP conditions;¹² IPA was selected due to its well known behaviour as a theta solvent for *p*(*n*BuMA). Other homogeneous alcoholic polymerisations of hydrophobic monomers include methyl methacrylate (MMA) in ethanol¹³ and 2-hydroxypropyl methacrylate (HPMA) in MeOH. In the latter case, *p*(HPMA) is soluble in MeOH⁹ and a range of linear homo/copolymers and complex architectures have been controllably produced using Cu(I) catalysed ATRP techniques including ¹⁴C-radiolabelled homopolymers,^{14,15} linear and branched copolymers^{16,17} and hyperbranched-polydendrons.^{18,19}

Recently we reported an interesting observation that ATRP of *n*BuMA could be conducted homogeneously at temperatures ≥ 25 °C in anhydrous MeOH; high monomer conversions were observed without any sign of precipitation during the reaction,²⁰ and very narrow dispersities ($\bar{D} = 1.02 - 1.13$) were obtained for polymers with number average degrees of polymerisation (DP_n) ≥ 500 monomer units. Our studies suggested that at low conversion, the monomer/methanol mixture was able to act as a good solvent for the propagating polymer chains and when conducted at elevated temperatures, the polymerisation was able to remain homogeneous at near complete conversion when held above the previously unreported cloud point temperature of *p*(*n*BuMA) in methanol. At near ambient temperatures and high conversion the polymers remained in solution, however, they were very sensitive to perturbation, for example rapid precipitation was seen during sampling for kinetics studies.

Homopolymers of hydrophilic monomers, such as 2-hydroxyethyl acrylate, and block copolymers containing monomers such as *N*-isopropylacrylamide and acrylic acid have also been homogeneously polymerised under alcoholic conditions using reversible addition-fragmentation chain transfer (RAFT) polymerisation.^{21,22} RAFT polymerisation-induced self-assembly, using ethanol as a poor solvent, was recently reported to generate phase separating systems during the polymerisation of alcohol soluble-alcohol insoluble A-B block copolymers,²³ facilitating access to various structures within complicated phase space. To the best of our knowledge, the homogeneous polymerisation of hydrophobic monomers in alcoholic media using RAFT has not been reported.

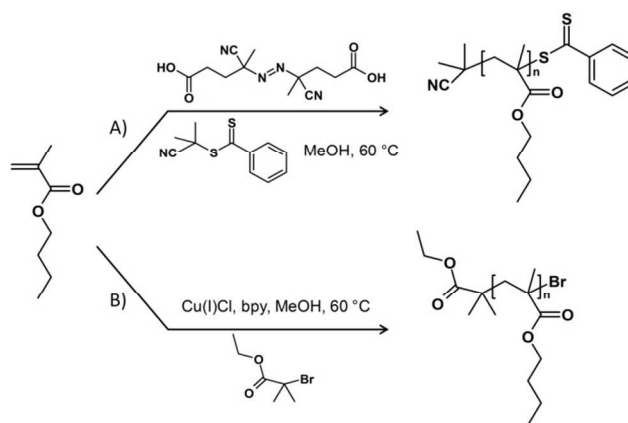
Our previous studies of homogeneous *p*(*n*BuMA) ATRP suggested a complex mechanism that was not solely related to the monomer/methanol mixed solvent conditions, but was possibly conditional on the monomer and polymerisation technique. Herein, we have developed our initial report to include: a comparison of methanolic ATRP of *n*BuMA with methanolic RAFT under very similar conditions, the formation of amphiphilic block copolymers with remarkably low dispersities, the synthesis of branched amphiphilic A-B block copolymers and the extension of monomer chemistry to include homopolymers and statistical copolymers containing MMA and *t*BuMA.

Results and Discussion

Comparison of RAFT and Cu(I)-catalysed ATRP in the methanolic polymerisation of *n*BuMA, *t*BuMA and MMA.

In our recent report of the ATRP of *n*BuMA in MeOH we demonstrated successful, homogeneous polymerisation to high conversion and very low \bar{D} across a temperature range extending from 25 °C to 60 °C using ethyl α -bromoisobutyrate (EBiB) as the initiator. Initial mechanistic studies, aimed at varying ligand chemistry and utilising conditions that would promote single-electron transfer living radical polymerization (SET-LRP), showed a loss of control compared to Cu(I)Cl/bipyridyl (bpy) catalysis. The role of Cu(0) was also qualitatively evaluated and no benefit was seen, leading us to conclude that the observed behaviour was potentially analogous to nanoprecipitation or polymerisation-induced self-assembly; a slow progression from a good solvent environment at low conversion (monomer + MeOH) through to a poor solvent at high conversion (MeOH) leading to propagation continuing within monomer-swollen collapsed polymer coils. In this case, the balance between the polymer-solvent interactions and the propagation equilibrium, controlled to some extent by the ligand chemistry and ratio of Cu oxidation states, appears to allow excellent control in MeOH through the Cu(I)Cl/bpy catalytic system.

To investigate this further, the non-catalytic controlled radical polymerisation technique RAFT was chosen to study the *n*BuMA polymerisation in anhydrous MeOH in the absence of the copper catalyst. Matching the exact conditions of an ATRP with RAFT polymerisation is not possible, especially at low temperatures, but as the ATRP of *n*BuMA had been successful at 60 °C, we selected a RAFT polymerisation utilising 2-cyano-2-propyl benzodithioate (CPBD) as the RAFT chain transfer agent (CTA) and 4,4'-azobis(4-cyanopentanoic acid) (ACVA) as the free radical initiator, Scheme 1. Polymerisations were conducted at 50 wt% monomer with respect to solvent.



Scheme 1. Controlled radical polymerisation of *n*BuMA conducted in anhydrous methanol at 60 °C using; A) RAFT with 4,4'-azobis(4-cyanopentanoic acid) and 2-cyano-2-propyl benzodithioate, and B) ATRP using ethyl α -bromoisobutyrate and a Cu(I)Cl/Bpy (1/2) catalytic system.

Despite the common mechanistic feature of an active/dormant chain equilibrium, RAFT and ATRP have considerable differences including the need for a specific source of free radicals, the rapid trapping of radicals by the CTA, and the close proximity of two separate propagating polymer chain ends to undergo CTA exchange. In contrast, ATRP requires the movement of a relatively small species, the Cu^{II} /ligand complexes, between active and dormant chains. The methanolic ATRP of *n*BuMA at 60 °C led to high conversions but relatively slow polymerisation, Table 1. Despite maintenance of controlled conditions, the formation of chains with high DP_n (> 200 monomer units) required prolonged reaction times; however, low \bar{D} values were achieved up to $\text{DP}_n = 500$.

Surprisingly, the RAFT polymerisation of *n*BuMA in MeOH was also highly successful, allowing high conversion, targeting of chains with DP_n up to 800 monomer units with low \bar{D} (1.06 – 1.12) over much shorter reaction times than ‘equivalent’ ATRP reactions; ATRP synthesis of a target $p(n\text{BuMA})_{1000}$ required 27 days at 60 °C to reach 50 % monomer conversion (ie $p(n\text{BuMA})_{500}$) but RAFT polymerisation with the same target DP_n achieved 80 % conversion (ie $p(n\text{BuMA})_{800}$) in just 44 hours. This suggests that the ATRP mechanism is not critical to the methanolic polymerisation and, indeed, leads to a slower propagation rate. Accurate number average molecular weight (M_n) targeting via RAFT was also improved over ‘equivalent’ ATRP reactions.

Table 1: Methanolic RAFT and Cu-catalysed methanolic ATRP of *n*BuMA at 60 °C

Target ^d DP_n	Conversion (%)	Time (hrs)	M_n Theory ^b	M_n ¹ H NMR	SEC (THF) ^c		
					M_n (g/mol)	M_w (g/mol)	\bar{D}
RAFT							
60	95	24	8100	10600	9300	10350	1.12
100	91	24	12950	15900	14550	15650	1.08
500	93	44	66150	83000	64750	70550	1.09
1000	80	44	113750	135900	107950	113950	1.06
ATRP^d							
60	99	55	8650		13600	13950	1.03
100	95	79	13700		19700	20300	1.03
500	66	235	47100		55550	61950	1.12
1000	50	648	71300		75900	85500	1.13
<i>p</i> (styrene) Std.e	-	-	9200 ^e		9300	9600	1.03

^a Target DP_n calculated as $[n\text{BuMA}]/[\text{initiator or CTA}]$; ^b Theoretical M_n includes initiator/CTA residue and was calculated as $[(\text{Target } \text{DP}_n \times 142.2 \text{ g/mol}) \times \text{experimental monomer conversion}]$; ^c SEC utilising THF eluent and $dn/dc = 0.0762 \text{ mL/g}$ (averaged across 18 samples); ^d see ref 20

Triple detection, size exclusion chromatography analysis (SEC, THF eluent), Figure 1A, showed the molecular weight distributions to be uniform and monomodal, even at high targeted DP_n . Visual observation of the ongoing RAFT polymerisations, a difficult study to achieve during ATRP due to the dark colour of the Cu(I) catalyst, showed homogeneous polymerisation at 60 °C when targeting $p(n\text{BuMA})_{60}$ through to high conversion; homogeneous reactions were observed when

targeting chain lengths of $\text{DP}_n \geq 100$ monomer units up to monomer conversions < 90 %, Figure 1Bi, after which the reactions became turbid, Figure 1Bii. If stirring was ceased, whilst maintaining reaction temperature, two phases appeared with a clear polymer rich-phase underneath a MeOH rich turbid phase; as determined by ¹H nuclear magnetic resonance (NMR) spectroscopy of each phase, Figure 1Biii (ESI Figure S3); samples were treated with THF to form homogeneous solutions before analysis. On cooling slightly below the $p(n\text{BuMA})/\text{MeOH}$ cloud point, the polymer-rich zone also phase separated, Figure 1Biv; complete phase separation was seen after leaving the polymerisation to stand at ambient temperature overnight (clear MeOH layer), Figure 1Bv.

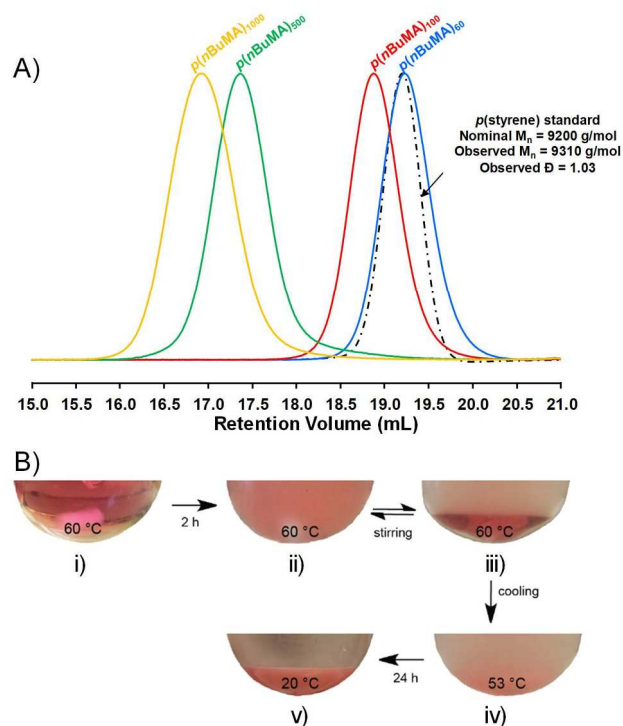


Figure 1. RAFT polymerisation of *n*BuMA in anhydrous methanol at 60 °C using CPBD and ACVA. A) SEC chromatograms (RI) showing *p*(*n*BuMA) molecular weight distributions across targeted $\text{DP}_n = 60$ -1000 monomer units – *p*(styrene) calibration standard shown for comparison; B) Photographs of the RAFT polymerisation showing - i) homogeneous polymerisation at 60 °C at low conversion, ii) onset of turbidity at high monomer conversions, iii) separation without stirring leaving a methanol-rich phase (top) and a polymer-rich phase (bottom) above the cloud point temperature, iv) precipitation of polymer upon cooling below the cloud point temperature (image taken at 53 °C), and v) complete phase separation and sedimentation at ambient temperature.

The onset of turbidity within the RAFT reactions did present the potential for pseudo-dispersion polymerisation conditions, as employed in polymerisation-induced self-assembly studies and we, therefore, expected a change in the rate of polymerisation if this was the case. As mentioned previously, the repeated sampling of methanolic ATRP polymerisations of *n*BuMA was often hampered by phase separation when the propagating solution was perturbed. We therefore chose to conduct RAFT kinetic studies using the simultaneous reaction of multiple vials containing monomer/CTA/initiator/MeOH

stock solutions; each vial was used to indicate a separate time-point within the overall polymerisation reaction and avoided sampling. Two kinetic studies were conducted using this technique, targeting $p(n\text{BuMA})_{100}$ and $p(n\text{BuMA})_{1000}$, Figure 2.

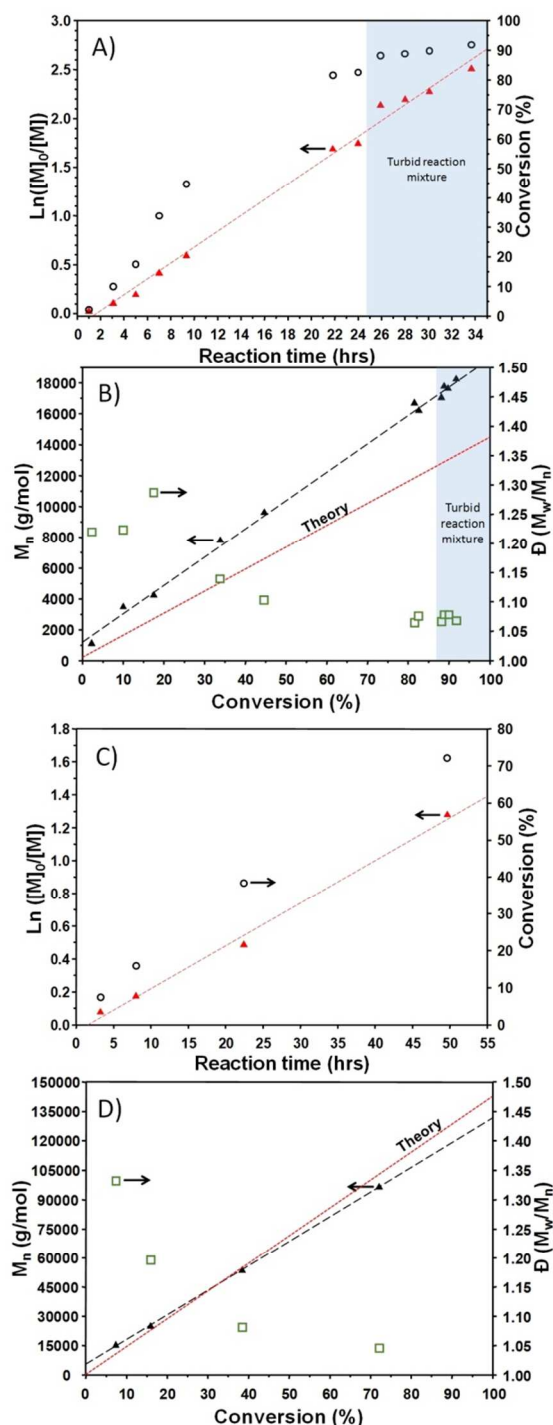


Figure 2. Kinetic studies for RAFT polymerisation of $n\text{BuMA}$ in anhydrous methanol at $60\text{ }^\circ\text{C}$ using CPBD and ACVA. Conversion and semi-logarithmic plots vs time, and evolution of M_n and dispersity with conversion for target $\text{DP}_n = 100$ monomer units (A and B) and $\text{DP}_n = 1000$ monomer units (C and D).

When targeting $p(n\text{BuMA})_{100}$, Figure 2A&B, the samples taken at relatively low conversion were homogeneous and a

steady increase in conversion and M_n , and a linear semi-logarithmic relationship, was observed as expected for controlled radical polymerisation. After approximately 24 hours, equating to 87 % monomer conversion, the remaining sample vials became turbid; analysis of these four vials showed no out-of-trend M_n values or any change in slope of the semi-logarithm plot. The kinetic study targeting $p(n\text{BuMA})_{1000}$, Figure 2C&D, maintained homogeneity up to the last data point, taken at 72 % conversion. The lack of turbidity in this case is presumably due to the remaining unreacted monomer acting as a co-solvent. The absence of any noticeable effect on the polymerisation after the onset of turbidity suggests that cosolvency is not critical to the RAFT reaction.

Having established that the controlled radical polymerisation of $n\text{BuMA}$ in MeOH was applicable to two different polymerisation mechanisms, the potential to extend beyond $n\text{BuMA}$ was investigated by conducting ATRP and RAFT polymerisations of MMA in MeOH under identical conditions to $n\text{BuMA}$ reactions, Table 2.

Table 2: Methanolic RAFT and Cu-catalysed methanolic ATRP of MMA and $t\text{BuMA}$ at $60\text{ }^\circ\text{C}$

Target DP_n	Conversion (%)	Time (hrs)	M_n Theory ^b	M_n ¹ H NMR	SEC (THF) ^c		
					M_n (g/mol)	M_w (g/mol)	\bar{D}
MMA RAFT							
60	95	25	5950	6400	7700	8400	1.10
100	93	27	9550	10600	11150	11900	1.07
200	89	25	18850	18750	21050	22550	1.07
ATRP							
60	99+	26	6150	-	8350	9950	1.19
100	98	23	10000	-	12050	13400	1.11
$t\text{BuMA}$ ATRP							
80	41	25	4800	-	5900	7800	1.32

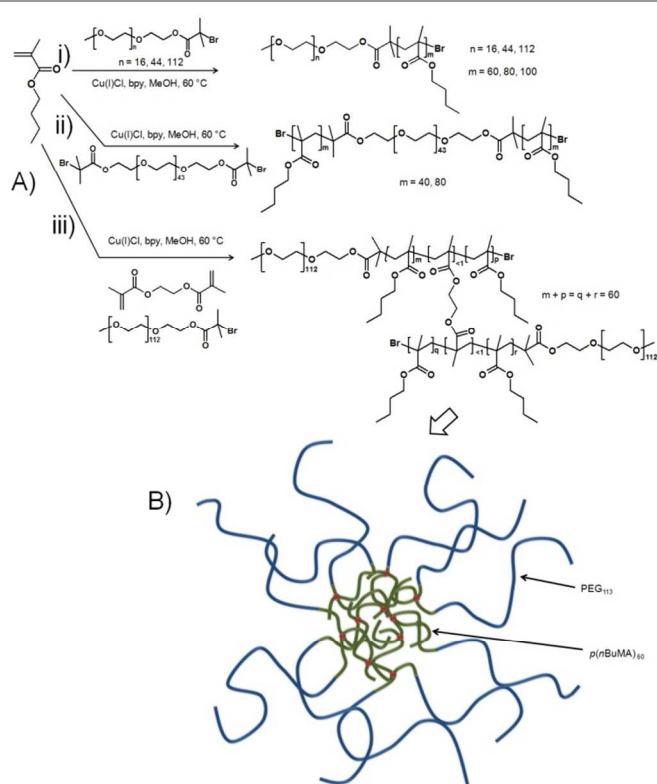
^a Target DP_n calculated as $[\text{monomer}]/[\text{initiator or CTA}]$; ^b Theoretical M_n includes initiator residue and was calculated as $[(\text{Target } \text{DP}_n \times (100.12 \text{ or } 142.2) \text{ g/mol}) \times \text{experimental monomer conversion}]$; ^c SEC utilising THF eluent and $dn/dc = 0.084 \text{ mL/g}$ for MMA (averaged across 6 samples; ESI Table S1)

Surprisingly, both methanolic RAFT and Cu-catalysed ATRP were able to generate low dispersity linear $p(\text{MMA})$ homopolymers (ESI Figure S4-5) to high conversion at $60\text{ }^\circ\text{C}$ despite again observing turbidity when targeting $\text{DP}_n \geq 100$ monomer units. The exploration of compatible monomer chemistry was also extended to $t\text{BuMA}$ using ATRP conditions, Table 2 (ESI Figure S6), and successful homogeneous polymerisation was observed but this was comparatively slow and led to much broader dispersity. No further homopolymerisation studies of $t\text{BuMA}$ were conducted.

Synthesis of amphiphilic linear and branched statistical A-B block copolymers via Cu(I)-catalysed methanolic ATRP.

The ready synthesis of a range of polyethylene glycol ATRP macroinitiators ($\text{PEG}_x\text{-Br}$), led to the choice of methanolic

ATRP for the evaluation of amphiphilic A-B block copolymer synthesis containing *p*(*n*BuMA) block segments, Scheme 2.



Scheme 2. Methanolic ATRP of *n*BuMA using PEG_{*x*}-Br macroinitiators. A) Reaction scheme detailing the syntheses of: i) amphiphilic linear A-B diblock copolymers, ii) amphiphilic linear A-B-A triblock copolymers, and iii) amphiphilic branched A-B block copolymers. B) Schematic representation of a branched PEG₁₁₃-*p*(*n*BuMA)₆₀-co-EGDMA_{0.9} block copolymer (branching points highlighted in red).

Three monofunctional macroinitiators were synthesised using reported techniques with DP_n = 17, 45 and 113 ethylene oxide repeat units. An α,ω -bifunctional macroinitiator with a DP_n = 91 monomer units was also synthesised (ESI Figure S7-9). After purification, SEC analysis (DMF eluent) of the macroinitiators showed narrow dispersity materials with measured M_n correlating well with theoretical values given for the commercial material, Table 3. Amphiphilic linear A-B and A-B-A block copolymers, and branched A-B block copolymers were targeted using the methanol at 60 °C, with varying PEG and *n*BuMA chain lengths, Scheme 2.

As would be expected, the PEG_{*x*}-Br macroinitiators were all fully soluble in MeOH with gentle warming and addition of the *n*BuMA monomer had no observable negative effect. This polymerisation system was able to generate very low dispersity amphiphilic A-B and A-B-A block copolymers, Table 3, across the different PEG chain lengths and for *p*(*n*BuMA) block lengths up to 100 monomer units. Although the *p*(*n*BuMA)_{*x*} block segments were larger than targeted, estimations of initiator efficiencies through a simple ratio of (Theoretical M_n)/(Observed M_n(SEC)) x 100 % gave consistent values across polymers formed from the different macro-initiators PEG₁₇-Br = 55 %, PEG₄₅-Br = 60 %, PEG₁₁₃-Br = 73 %, Br-

PEG₉₁-Br = 70 %, with a maximum standard deviation (σ) = 3 % observed for PEG₁₁₃-Br.

Table 3: Methanolic Cu-catalysed ATRP of *n*BuMA at 60 °C using PEG-derived macroinitiators

Theoretical/ Target ^a / DP _n	Conv. (%)	Time (hrs)	M _n Theory ^b	M _n ¹ H NMR	SEC (DMF)		
					M _n (g/mol)	M _w (g/mol)	Đ
PEG-macro initiators							
PEG ₁₇	-	-	900	950	-	-	-
PEG ₄₅	-	-	2150	2300	2300	2500	1.09
PEG ₉₁	-	-	4300	4650	5150	5400	1.05
PEG ₁₁₃	-	-	5150	5800	6000	6150	1.02
PEG₁₇-Br							
60	99	24	9350	15550	17850	18250	1.02
80	96	24	11850	19100	21300	21700	1.02
100	92	24	14000	23200	24900	25400	1.02
PEG₄₅-Br							
60	99	24	10600	15950	17250	17900	1.04
80	98	25	13250	18800	23000	24050	1.05
100	97	27	15900	29600	26800	27800	1.04
PEG₁₁₃-Br							
60	97	5	13420	12400	17650	18050	1.02
80	93	17	15800	12400	21850	22500	1.03
100	94	17	18600	16100	26600	27700	1.04
Br-PEG₉₁-Br							
40 (x2)	99	26	15600	-	22050	26000	1.18
80 (x2)	98	26	26600	-	38300	38300	1.13

^a Target DP_n calculated as [*n*BuMA]/[initiator]; ^b Theoretical M_n includes initiator residue and was calculated as [(Target DP_n x 142.2 g/mol) x experimental monomer conversion]

Kinetic studies of the individual macroinitiated polymerisations showed well controlled conditions. The value of the refractive index increment (dn/dc) of the individual copolymer samples, taken during the kinetic studies, are expected to vary systematically due to the progressively increasing *p*(*n*BuMA) chain at the end of each PEG_{*x*}-Br macroinitiator and the range of different targeted hydrophobic block lengths. M_n determination using SEC, employing the dn/dc value from the final recovered polymer calculated by the triple detection SEC instrument (ESI Figure S10, S13, S15 & S17), was compared with M_n values using theoretical copolymer dn/dc values, calculated for each kinetic point using Equation 1, discussed by Hadjichristidis *et al.*²⁴

$$\left(\frac{dn}{dc}\right)_{\text{Copolymer}} = W_{\text{PEG}}\left(\frac{dn}{dc}\right)_{\text{PEG}} + (1 - W_{\text{PEG}})\left(\frac{dn}{dc}\right)_{p(n\text{BuMA})} \quad [1]$$

where W_{PEG} is the weight fraction of the PEG_{*x*} block and $(dn/dc)_{\text{PEG}}$ and $(dn/dc)_{p(n\text{BuMA})}$ values determined by taking the average values calculated by triple detection SEC (DMF) for three linear homopolymer samples of each polymer; $(dn/dc)_{\text{PEG}} = 0.0566 \text{ mL/g}$ ($\sigma = 0.0010$), $(dn/dc)_{p(n\text{BuMA})} = 0.0624 \text{ mL/g}$ ($\sigma = 0.0007$), (ESI Table S2).

The comparative M_n vs. conversion graphs for targeted copolymers showed a decreasing discrepancy with increasing

PEG macroinitiator chain length (Figure 3, ESI Figure S11-12, S14 & S16) as may be expected due to the increasing weight fraction dominance of the PEG_x macroinitiator chains.

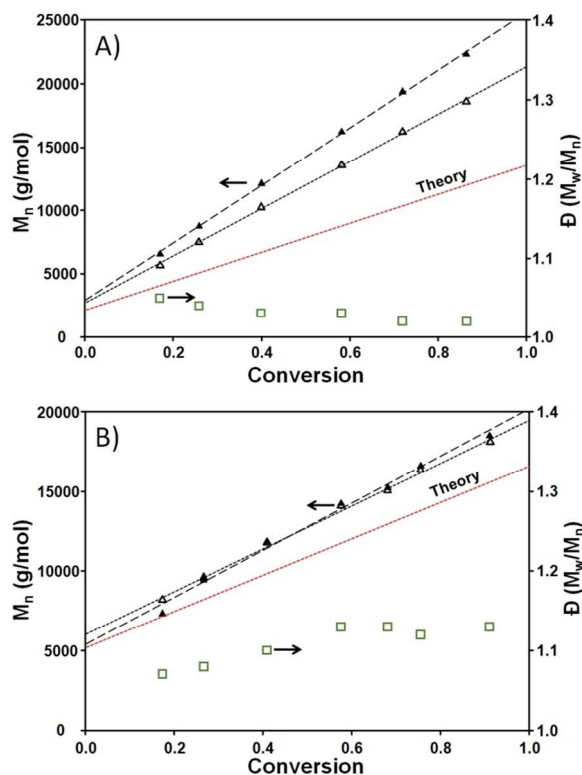


Figure 3. Kinetic studies anhydrous methanolic ATRP at 60 °C showing the evolution of M_n and dispersity with conversion for PEG_x-*p*(*n*BuMA)₈₀ block copolymers. A) Polymerisation initiated with PEG₄₅-Br macroinitiator, and B) polymerisation initiated with PEG₁₁₃-Br macroinitiator. Conversion vs M_n plotted using both dn/dc value of the final purified polymer (solid triangles) and calculated dn/dc using equation [1] (open triangles); dispersity shown as open green squares.

The PEG₁₁₃-Br macroinitiator was chosen to study the formation of *p*(PEG₁₁₃-*block*-MMA_x) A-B block copolymers under methanolic ATRP conditions at 60 °C to establish the dependence on hydrophobic monomer chemistry. By simply substituting MMA for *n*BuMA to match earlier reactions, *p*(MMA) block lengths of 60, 80 and 100 monomer units were targeted. Conversions > 99 % were obtained, requiring increasing reaction times dependent on the DP_n of the targeted hydrophobic *p*(MMA) block, Table 4. SEC (DMF) analysis, showed unimodal molecular weight distributions (ESI Figure S18) and higher \bar{D} values than the corresponding *p*(*n*BuMA) containing block copolymers. Targeting of overall block copolymer M_n was relatively accurate, compared to the polymerisation of *n*BuMA, Table 3, and macroinitiator efficiency was calculated as approximately 82.5 % ($\sigma = 6\%$) across the three copolymerisations. The improved macroinitiator efficiency may be due to the varying monomer/methanol solvation of the PEG chains and will have improved the ability to target M_n , however, the long reaction times and increased \bar{D} leads to a clear compromise within the

choice of monomer chemistry. It is unclear at this stage whether this compromise can be overcome by termination at lower conversions as these polymerisations were allowed to progress to near completion.

Branched copolymerisation of *n*BuMA with ethylene glycol dimethacrylate (EGDMA) was also attempted using the PEG₁₁₃-Br macroinitiator, at ratios of EGDMA:PEG₁₁₃-Br of < 1:1, Scheme 2Aiii & 2B. This approach to branched vinyl polymerisation was pioneered by Sherrington and co-workers,²⁵⁻²⁸ initially through the use of conventional free radical polymerisation utilising thiol chain transfer agents,^{29,30} and latterly through group transfer polymerisation³¹ and various controlled radical approaches.^{32,33}

Table 4: Methanolic Cu-catalysed ATRP of MMA at 60 °C using PEG₁₁₃-Br

Target ^a DP _n	Conv. (%)	Time (hrs)	M_n Theory ^b	M_n ¹ H NMR	SEC (DMF)		
					M_n (g/mol)	M_w (g/mol)	\bar{D}
PEG₁₁₃-Br							
60	99+	29	11100	11250	14600	17000	1.16
80	99+	49	13100	12050	14900	18200	1.22
100	99+	67	15100	15050	18200	22300	1.23

^a Target DP_n calculated as [MMA]/[initiator]; ^bTheoretical M_n includes initiator residue and was calculated as [(Target DP_n × 100.12 g/mol) × experimental monomer conversion]

As has been reported previously for different branched vinyl polymerisations, the formation of high molecular weights within such reactions are achieved at conversions > 85 %.^{34,17} Each polymerisation was, therefore, allowed to reach approximately 99 % conversion, requiring longer reaction times than the equivalent linear *p*(PEG₁₁₃-*block*-*n*BuMA₆₀) syntheses. At EGDMA:PEG₁₁₃-Br molar ratios between 0.75:1 and 0.9:1, branched copolymers with M_n and M_w values exceeding the linear materials were generated with dispersities that are typical of this type of reaction, Table 5. An increasingly complex molecular weight distribution was observed during SEC analyses, Figure 4, and values of \bar{D} increased with increasing EGDMA, mirroring the increasing M_w values.

Table 5: Methanolic Cu-catalysed ATRP copolymerisation of *n*BuMA and EGDMA at 60 °C using PEG₁₁₃-Br

Target ^a DP _n	Conv. (%)	Time (hrs)	EGDMA: PEG ₁₁₃ -Br	SEC (DMF)		
				M_n (g/mol)	M_w (g/mol)	\bar{D}
PEG₁₁₃-Br						
60	99	53	0.95:1	36400	439550	12.08
60	99	51	0.9:1	161500	2327000	14.41
60	99	51	0.85:1	36600	419500	11.46
60	99	51	0.8:1	27800	184750	6.62
60	99	48	0.75:1	34100	186200	5.46

^a Target DP_n calculated as [*n*BuMA]/[initiator]

At EGDMA:PEG₁₁₃-Br ratio > 0.9:1, a decrease in M_w was observed (ESI Figure S19), indicating the formation of microgel and the removal of very high molecular weight swollen materials during the filtration step during analytical

sample preparation or when removing the catalytic system from the crude polymer sample; the $dndc$ values obtained during analysis of each polymer in Table 5 were consistent, therefore suggesting removal of microgel during purification (alumina column) of the crude polymer (ESI Table S3).

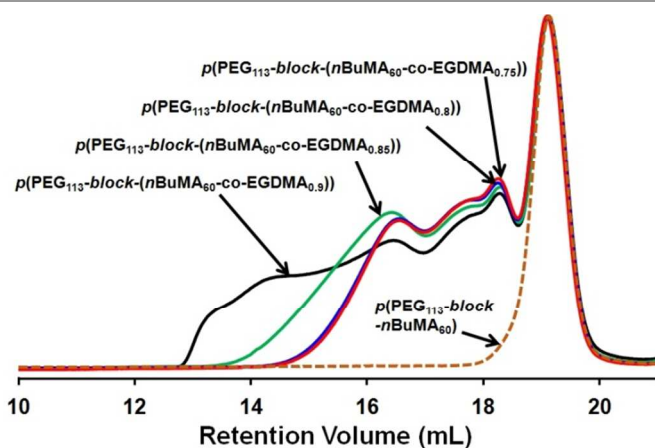


Figure 4. Overlaid SEC chromatograms (RI) of linear and branched A-B block copolymers produced using methanolic ATRP of *n*BuMA at 60 °C (targeting DP_n , 60 monomer units within the hydrophobic block) using PEG₁₁₃-Br macroinitiator and varying equivalents (0.75-0.9 wrt. initiator) of divinyl monomer, EGDMA.

Overlaid SEC chromatograms of each branched amphiphilic A-B block copolymer with the linear $p(\text{PEG}_{113}\text{-block-}n\text{BuMA}_{60})$, Figure 4, showed the expected presence of linear chains that have not been incorporated into the branched architecture. This also confirmed the formation of primary A-B block copolymer chains equivalent in dispersity and molecular weight to the linear polymer analogues, as shown in previous reports. The sample formed at a ratio of 0.9:1, therefore, contains number average structures with approximately 9 conjoined primary amphiphilic A-B block copolymer chains and weight average structures containing approximately 129 primary chains. At lower ratios, the number average structures contain approximately 2 primary chains with weight average structures varying from approximately 10 – 23 primary chains.

Our previous study of *n*BuMA ATRP in MeOH showed that successful homopolymerisation could also be achieved at 25 °C, therefore a study to establish the potential for A-B block copolymer synthesis using ATRP at reduced temperature was conducted using the three PEG_x-Br macroinitiators and targeting a chain length of 80 *n*BuMA units; MMA block copolymerisation at this temperature was also studied using PEG₁₁₃-Br and targeting a $p(\text{MMA})$ block length of 80 monomer units.

The macroinitiated polymerisations were allowed to react for approximately 25 hours to allow a comparison of the different initiators and monomers used. Monomer conversion appeared to increase with PEG_x-Br chain length within the *n*BuMA polymerisations with PEG₁₇-Br reaching the lowest value. SEC analysis of the $p(\text{PEG}_x\text{-block-}n\text{BuMA}_{80})$ copolymers (ESI Figure S20) showed better targeting of M_n using the longer macroinitiators and estimations of macroinitiator efficiencies of PEG₁₇-Br = 64 %,

PEG₄₅-Br = 86 %, PEG₁₁₃-Br = 92 %. All macroinitiators appear, therefore, to be more efficient at lower temperature; however, higher dispersities were seen for all recovered block copolymer samples when compared to the materials synthesised at 60 °C. In contrast, MMA polymerised in a very similar manner at both temperatures when using PEG₁₁₃-Br (ESI Figure S21), yielding A-B block copolymers with similar \bar{D} values, achieving similar conversions and maintaining a high initiator efficiency of approximately 97 %. As with *n*BuMA, an improvement in estimated initiator efficiency was seen at 25 °C when using MMA. This may indicate the avoidance of radical termination at low temperatures during the early stages of the ATRP reaction, with modification of initiation/propagation and reduced termination as the redox equilibrium evolves.

Table 6: Synthesis of amphiphilic A-B block copolymers using PEG_x-Br macroinitiators and either *n*BuMA or MMA *via* methanolic Cu-catalysed ATRP at 25 °C: Hydrophobic block target DP_n = 80 monomer units.

Initiator	Conv. (%)	Time (hrs)	M_n Theory ^a	M_n ¹ H NMR	SEC (DMF)		\bar{D}
					M_n (g/mol)	M_w (g/mol)	
<i>n</i>BuMA							
PEG ₁₇ -Br	68	25	8600	7900	13550	16300	1.20
PEG ₄₅ -Br	89	25	12300	13100	14250	18800	1.32
PEG ₁₁₃ -Br	85	26	14850	14950	16200	19500	1.21
MMA							
PEG ₁₁₃ -Br	91	27	12400	12950	12800	15750	1.23

^a Theoretical M_n includes initiator residue and was calculated as [(Target DP_n × (100.12 or 142.2) g/mol) × experimental monomer conversion]

Synthesis of hydrophobic linear statistical copolymers via Cu(I)-catalysed methanolic ATRP.

The success of the ATRP-derived branched EGDMA/*n*BuMA statistical copolymers led us to consider the formation of hydrophobic statistical copolymers from the three monomers that we had studied; *n*BuMA, *t*BuMA and MMA. EBIB was used to initiate three statistical copolymerisations at 60 °C, comprising a 1:1 ratio of MMA, *n*BuMA or *t*BuMA and targeting DP_n = 60 for each comonomer (overall copolymer DP_n = 120 monomer units), Table 7. The reactions were left to react for various times to allow high overall combined conversions as monitored by ¹H NMR.

¹H NMR and SEC analysis (ESI Figure S22-24) of the reactions and final polymers allowed a number of observations. The inclusion of *n*BuMA into an MMA or *t*BuMA polymerisation appears to decrease the measured \bar{D} values relative to the closest homopolymerisations conducted during this study, Table 2. Dispersity values indicating increased control were also possible when targeting an MMA-rich statistical copolymer containing very small amounts of *n*BuMA, as can be seen through comparisons of $p(\text{MMA}_{60}\text{-stat-}n\text{BuMA}_{10})$ (\bar{D} = 1.09) with $p(\text{MMA})_{60}$ (\bar{D} = 1.19) and $p(\text{MMA})_{100}$ (\bar{D} = 1.11). In the case of *t*BuMA/*n*BuMA statistical copolymerisation, extended reaction times were required but appreciable conversion of both monomers was

achieved, leading to a narrow dispersity copolymer with much greater control than *t*BuMA homopolymerisation under similar conditions. A 1:1 statistical copolymer of *t*BuMA and MMA required very long reaction times to reach individual monomer conversions of approximately 50 % and a much higher dispersity was observed than seen for either homopolymerisation (ESI Figure S24).

Table 7: Synthesis of statistical copolymers containing mixtures of MMA, *n*BuMA and *t*BuMA using methanolic Cu-catalysed ATRP at 60 °C.

Target Copolymer Composition	Comonomer Conv. (%)	Time (hrs)	M_n Theory ^b	SEC (THF)		
				M_n (g/mol)	M_w (g/mol)	\bar{D}
MMA ₆₀ / <i>n</i> BuMA ₆₀	MMA(90)/ <i>n</i> BuMA(94)	43	13600	19000	21400	1.13
MMA ₆₀ / <i>n</i> BuMA ₁₀	MMA(99)/ <i>n</i> BuMA(99)	24	7550	11000	12050	1.09
<i>t</i> BuMA ₆₀ / <i>n</i> BuMA ₆₀	<i>t</i> BuMA(76)/ <i>n</i> BuMA(89)	72	14100	18500	20400	1.11
<i>t</i> BuMA ₆₀ /MMA ₆₀	<i>t</i> BuMA(57)/MMA(43)	141	7450	9800	14200	1.45

^a Target DP_n calculated as [individual monomer]/[initiator]; ^b Theoretical M_n includes initiator residue and was calculated as [(Target DP_n x individual monomer molecular weights) x individual experimental monomer conversions]

Conclusions

We aimed to expand our initial report of controlled, homogeneous ATRP polymerisation of *n*BuMA using MeOH, a known anti-solvent for *p*(*n*BuMA). The demonstration of successful ATRP and RAFT suggests the reaction conditions dominate this approach, rather than the polymerisation technique and mechanism, which was not clear previously. A number of mechanistic questions are raised for the RAFT examples under these conditions, as the proximity and accessibility of propagating polymer chain ends is highly important for RAFT, our reactions are particularly slow and they do not require additional ACVA.

At low conversion the monomer/MeOH reaction mixture is able to considerably decrease the MeOH cloud point *p*(*n*BuMA) homopolymers,²⁰ although we have clearly shown this to be dependent on DP_n. As RAFT homopolymerisations became turbid at *high* conversion when targeting DP_n values ≥ 100 , this may indicate that at least a fraction of the propagating chains had phase-separated within the poor solvent conditions (low monomer concentration); however, the lack of phase-separation for lower targeted DP_n values and the coexistence of a polymer-rich homogeneous phase with the polymer-poor turbid phase at high conversion, suggests that the observed turbidity may originate from a relatively low concentration of chains that are within the intermediate dormant radical stage of the reversible fragmentation. Such radicals have been observed using ESR approaches³⁵ and an extended life-time for such intermediates may lead to the prolonged reactions we observe. Modification of the rate of fragmentation may also

explain the continued controlled polymerisation over our extended reaction times (>50 hours) despite reported RAFT. The authors do not know the ACVA half-life under these conditions (methanol/60 °C), but assuming the 10 hr half-life temperature is similar to that in water (69 °C), sufficient ACVA would be available after 50 hours to maintain the RAFT reaction if required.

ESR studies are needed to confirm this hypothesis, however, the intermediate dormant polymer radicals would temporarily have an effective chain length = $2 \times DP_n$, Figure 5, and, therefore, may have exceeded the phase boundary. At approximately 75 % conversion, the targeted RAFT of *p*(BuMA)₁₀₀₀ was still homogeneous, suggesting the monomer co-solvency effect has a significant impact on reaction success in addition to the elevated temperature. The lack of an observed change in the kinetics of the polymerisation after the onset of turbidity (high conversion) also supports homogeneous propagation conditions and a lack of direct relation between turbidity and the growing polymer; it is also possible that the CTA-terminated chain-end is preferentially solubilised by the methanolic environment.

Extending methanolic controlled polymerisation to MMA and *t*BuMA was a surprise to the authors, especially considering the high conversions and low \bar{D} at high solids content (50 wt%); *p*(MMA) of DP_n = 200 monomer units were achieved by RAFT, and 100 monomer units by ATRP; longer polymer chains may be achievable but we aimed solely to demonstrate successful polymerisation under these conditions. The ATRP of MMA has been shown in ionic liquids using an ionic liquid-derived initiator, 1-(2-bromoisobutyryloxyethyl)-3-methylimidazolium hexafluoro-phosphate ($\bar{D} = 1.18 - 1.31$).³⁶ The presence of the cationic imidazole derivative end group rendered *p*(MMA) soluble in MeOH at DP_n ≤ 50 monomer units, but the homopolymers synthesised here have no specific solubilising end group and M_n values up to four-fold higher than this previous study. Despite the anti-solvent nature of MeOH for *p*(MMA), comparative specular neutron reflectivity studies of deuterated-*p*(MMA) films³⁷ in contact with various alcohols showed MeOH exposure results in the most solvent penetration and film swelling. MeOH-swollen *p*(MMA) chains may, therefore, be present within these polymerisations, aided by unreacted monomer at lower conversions. This supports the solvent-swollen mechanism hypothesis described in our report of methanolic ATRP of *n*BuMA,²⁰ following the steps: 1) small oligomers generated homogeneously under good solvent conditions (monomer/MeOH), 2) gradual collapse of the chains during monomer depletion, 3) metastable solutions of propagating slightly-swollen coils. The observed sensitivity to perturbation would arise if local temperature fluctuations or impurities are introduced, leading to macrophase separation.

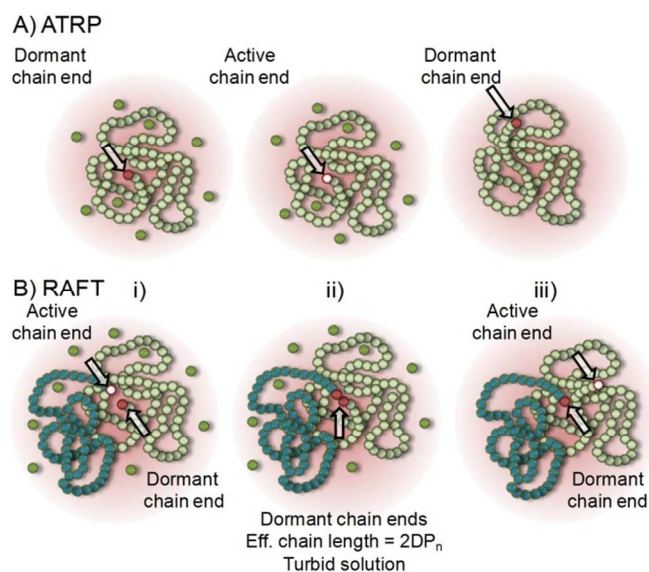


Figure 5. Schematic representation and contrast of ATRP and RAFT homogeneous polymerisation of *n*BuMA in methanol, showing the collapse of polymer chains during monomer depletion and metastable propagating solvent-swollen polymer coils. A) Polymerisation via ATRP: i) Dormant chain end at relatively high conversion, ii) active chain end after diffusion of catalyst, and iii) dormant chain end after monomer consumption. B) Polymerisation via RAFT: i) active and dormant chains at relatively high conversion, ii) dormant intermediate species during chain transfer with effective chain length = $2DP_n$, iii) generation of active chain and dormant chain after fragmentation.

A-B and A-B-A block copolymer synthesis using PEG_x-Br macroinitiators is, possibly, not that surprising, however, the narrow dispersity is remarkable for the materials containing *p*(*n*BuMA) block segments. Studies of crosslinked *p*(MMA) nanogel swelling in PEG/alcohol mixtures suggest hydrophobic complex formation and subsequent generation of a pseudo-good solvent conditions;³⁸ this was supported by radial distribution function calculations, characterising the proximity of oxygen atoms within the two 'solvent' components and *p*(MMA), and dynamic light scattering measurements in the presence of different PEG/alcohol mixtures. The block copolymerisations presented here may have benefitted from the local solvent environment generated by PEG/MeOH complex formation in addition to the MeOH solubility of the PEG block.

Finally, our statistical copolymerisation results do underline the ability to utilise *t*BuMA as a viable monomer in MeOH, although results were not as good as MMA and *n*BuMA. Reports of alcohol/acrylic ester hydrogen bonding suggest that both monomer and alcohol structure impact the interactions.³⁹ Although *t*-butyl esters were not studied in these reports, it can be assumed that the increased steric hinderance from the bulky tertiary ester may disturb interactions between the propagating chain with MeOH. Polymerisation of *t*BuMA was noticeably slower, and its presence within the statistical copolymerisations extended reaction times and decreased second monomer conversion. This suggests a slow propagation of *t*BuMA, and reduced rate of addition of MMA and *n*BuMA to polymer chains propagating from a *t*BuMA chain-end monomer residue.

Co-monomer conversions suggest relatively similar reactivity between the monomer pairs studied, including those containing *t*BuMA. There are relatively few ATRP reactivity ratio studies, but monomer pairs showing significant differences to data obtained with conventional free radical polymerisation have been reported,⁴⁰ whilst other reports suggest little variation of observed reactivity ratios between conventional and controlled radical polymerisations.⁴¹ Our statistical copolymerisation studies have not been conducted to accurately determine reactivity ratios but it does seem that controlled radical polymerisation within this set of hydrophobic monomers reacting via methanolic ATRP leads to $r_A \approx r_B$.

The flexibility and control demonstrated for a range of homopolymers and varying architectures using three hydrophobic monomers, suggests that this non-obvious reaction solvent choice may provide considerable scope for polymer synthesis. The copolymerisation of *t*BuMA has been shown several times to allow for post-polymerisation hydrolysis and introduction of methacrylic acid functionality.^{42,43} This may present significant potential for *t*BuMA copolymerisation under these reaction conditions, and further studies to generate acidic and ionic polymers with complex architectures are underway.

Acknowledgements

The authors would like to thank the Engineering and Physical Sciences Research Council for funding (EP/I038721/1). ABD is also grateful for a PhD studentship. The University of Liverpool and the Centre for Materials Discovery at Liverpool is also gratefully acknowledged for access to analytical techniques.

Notes and references

Department of Chemistry, University of Liverpool, Crown Street, L69 7ZD, UK. E-mail: srannard@liv.ac.uk

Electronic Supplementary Information (ESI) available: Experimental details, NMR spectra, additional SEC chromatograms, calculations of average dn/dc values, kinetic data. See DOI: 10.1039/b000000x/

- 1 a) H. Bergenudd, G. Coullerez, M. Jonsson, and E. Malmström, *Macromolecules*, 2009, **42**, 3302; b) A. Hirao, R. Goseki and Takashi Ishizone, *Macromolecules*, 2014, **47**, 1883; c) A. Sandeau, S. Mazières and M. Destarac, *Polymer*, 2012, **53**, 5601.
- 2 R. Mincheva, D. Paneva, L. Mespouille, N. Manolova, I. Rashkov and P. Dubois, *J. Polym. Sci. Pol. Chem.*, 2009, **47**, 1108.
- 3 K. Matyjaszewski, *J. Macromol. Sci. Pure*, 1997, **A34**, 1785.
- 4 N. M. L. Hansen, K. Jankova and S. Hvilsted, *Eur. Polym. J.*, 2007, **43**, 255.
- 5 K. Matyjaszewski and N. V. Tsarevsky, *J. Am. Chem. Soc.*, 2014, **136**, 6513.
- 6 T. G. Fox, J. B. Kinsinger, H. F. Mason and E. M. Schuele, *Polymer*, 1962, **3**, 71.
- 7 M. Long, S. H. Rogers, D. W. Thornthwaite, F. R. Livens and S. P. Rannard, *Polym. Chem.*, 2011, **2**, 581.
- 8 a) K. L. Robinson, M. V. de Paz-Báñez, X. S. Wang and S. P. Armes, *Macromolecules*, 2001, **34**, 5799; b) K. L. Robinson, M. A. Khan, M. V. de Paz Báñez, X. S. Wang and S. P. Armes, *Macromolecules*,

- 2001, **34**, 3155; c) S. Jana, S. P. Rannard and A. I. Cooper, *Chem. Commun.*, 2007, 2962; d) M. Save, J. V. M. Weaver and S. P. Armes, *Macromolecules*, 2002, **35**, 1152.
- 9 X. Bories-Azeau and S. P. Armes, *Macromolecules*, 2002, **35**, 10241.
- 10 L. S. Connell, J. R. Jones and J. V. M. Weaver, *Polym. Chem.*, 2012, **3**, 2735.
- 11 a) T. F. Finkler, S. Lucia, M. B. Dogru and S. Engell, *Ind. Eng. Chem. Res.*, 2013, **52**, 5906; b) C. Capello, U. Fischer and K. Hungerbühler, *Green Chem.*, 2007, **9**, 927.
- 12 S. McDonald and S. P. Rannard, *Macromolecules*, 2001, **34**, 8600.
- 13 S. K. Jewrajka, U. Chatterjee and B. M. Mandal, *Macromolecules*, 2004, **37**, 4325.
- 14 M. Long, D. W. Thornthwaite, S. H. Rogers, F. R. Livens and S. P. Rannard, *Polym. Chem.*, 2012, **3**, 154.
- 15 M. Long, D. W. Thornthwaite, S. H. Rogers, G. Bonzi, F. R. Livens and S. P. Rannard, *Chem. Commun.*, 2009, 6406.
- 16 a) Y. Li and S. P. Armes, *Macromolecules*, 2005, **38**, 8155; b) J. Ford, P. Chambon, J. North, F. L. Hatton, M. Giardiello, A. Owen, and S. P. Rannard, *Macromolecules*, 2015, **48**, 1883.
- 17 R. A. Slater, T. O. McDonald, D. J. Adams, E. R. Draper, J. V. M. Weaver and S. P. Rannard, *Soft Matter*, 2012, **8**, 9816.
- 18 F. L. Hatton, P. Chambon, T. O. McDonald, A. Owen and S. P. Rannard, *Chem. Sci.*, 2014, **5**, 1844.
- 19 F. L. Hatton, L. M. Tatham, L. R. Tidbury, P. Chambon, T. He, A. Owen and S. P. Rannard, *Chem. Sci.*, 2015, **6**, 326.
- 20 A. B. Dwyer, P. Chambon, A. Town, T. He, A. Owen and S. P. Rannard, *Polym. Chem.*, 2014, **5**, 3608.
- 21 J. T. Lai, D. Filla and R. Shea, *Macromolecules*, 2002, **35**, 6754.
- 22 C. M. Schilli, M. Zhang, E. Rizzardo, S. H. Thang, Y. K. Chong, K. Edwards, G. Karlsson and A. H. E. Müller, *Macromolecules*, 2004, **37**, 7861.
- 23 E. R. Jones, M. Semsarilar, A. Blanz and S. P. Armes, *Macromolecules*, 2012, **45**, 5091.
- 24 N. Hadjichristidis, S. Pispas and G. Floudas (2002), *Block Copolymers: Synthetic Strategies, Physical Properties, and Applications*, John Wiley & Sons, Inc., Hoboken, New Jersey, ISBN-13: 978-0471394365.
- 25 A. T. Slark, D. C. Sherrington, A. Titterton and I. K. Martin, *J. Mater. Chem.*, 2003, **13**, 2711.
- 26 F. Isaure, P. A. G. Cormack and D. C. Sherrington, *Macromolecules*, 2004, **37**, 2096.
- 27 F. Isaure, P. A. G. Cormack and D. C. Sherrington, *J. Mater. Chem.*, 2003, **13**, 2701.
- 28 S. Graham, S. P. Rannard, P. A. G. Cormack and D. C. Sherrington, *J. Mater. Chem.*, 2007, **17**, 545.
- 29 J. V. M. Weaver, S. P. Rannard, and A. I. Cooper, *Angew. Chem. Int. Ed.*, 2009, **48**, 2131.
- 30 J. V. M. Weaver, R. T. Williams, B. J. L. Royles, P. H. Findlay, A. I. Cooper and S. P. Rannard, *Soft Matter*, 2008, **4**, 985.
- 31 V. Bütün, I. Bannister, N. C. Billingham, D. C. Sherrington and S. P. Armes, *Macromolecules*, 2005, **38**, 4977.
- 32 J. Rosselgong and S. P. Armes, *Polym. Chem.*, 2015, **6**, 1143.
- 33 T. He, D. J. Adams, M. F. Butler, C. T. Yeoh, A. I. Cooper and S. P. Rannard, *Angew. Chem. Int. Ed.*, 2007, **46**, 9243.
- 34 I. Bannister, N. C. Billingham, S. P. Armes, S. P. Rannard and P. Findlay, *Macromolecules*, 2006, **39**, 7483.
- 35 D. G. Hawthorne, G. Moad, E. Rizzardo and S. H. Thang, *Macromolecules*, 1999, **32**, 5457.
- 36 S. Gong, H. Ma and X. Wan, *Polym. Int.*, 2006, **55**, 1420.
- 37 H. Atarashi, H. Morita, D. Yamazaki, M. Hino, T. Nagamura and K. Tanaka, *J. Phys. Chem. Lett.*, 2010, **1**, 881.
- 38 S. M. Lee, J. H. Lee and Y. C. Bae, *Fluid Phase Equilib.*, 2014, **382**, 107.
- 39 K. Dharmalingam, K. Ramachandran and P. Sivagurunathan, *Spectrochim. Acta A*, 2007, **66**, 48.
- 40 J. Lad, S. Harrison, G. Mantovani and D. M. Haddleton, *Dalton Trans.*, 2003, 4175.
- 41 S. B. Lee, A. J. Russell and K. Matyjaszewski, *Biomacromolecules*, 2003, **4**, 1386.
- 42 T. E. Long, R. D. Allen, and J. E. McGrath, *Synthesis and Characterization of Block Copolymers Containing Acid and Ionomeric Functionalities*. In *Chemical Reactions in Polymers*, J. L. Benham and J. F. Kinstle, Eds., ACS Symposium Series No. 364, Chapter. 19, 258.
- 43 S. P. Rannard, N. C. Billingham, S. P. Armes and J. Mykytiuk, *Eur. Polym. J.*, 1993, **29**, 407.

Graphical Abstract

Exploring the homogeneous controlled radical polymerisation of hydrophobic monomers in anti-solvents for their polymers: RAFT and ATRP of various alkyl methacrylates in anhydrous methanol to high conversion and low dispersity.

A. B. Dwyer, P. Chambon, A. Town, F. L. Hatton, J. Ford and S. P. Rannard*

ATRP and RAFT of hydrophobic monomers in anhydrous methanol, a traditional precipitant for the polymers, has been shown to form homopolymers, branched copolymers and statistical copolymers from nBuMA, MMA and tBuMA at 60 °C and 25 °C to very high conversion, high molecular weight ($DP_n = 800$ monomer units) and very low dispersities (as low as 1.02) without phase separation

